Binding site control in a layer-by-layer deposited chitosan–carbon nanoparticle film electrode

Liza Rassaei,[a] Michael J. Bonné,[b] Mika Sillanpää[a] and Frank Marken*[b]

Received (in Durham, UK) 8th January 2008, Accepted 13th February 2008
First published as an Advance Article on the web 26th March 2008
DOI: 10.1039/b800331a

Thin chitosan–carbon nanoparticle films (*ca.* 2 nm average thickness increase per layer) are assembled onto tin-doped indium oxide (ITO) electrode substrates in a layer-by-layer deposition process employing carbon nanoparticles of *ca.* 8 nm average diameter and an aqueous solution of chitosan (poly-D-glucosamine, low molecular weight, 75–85% deacetylated). Chitosan introduces amine/ammonium functionalities which are employed for the immobilization of redox systems (i) *via* physisorption of indigo carmine and (ii) *via* chemisorption of 2-methyleneanthraquinone. The number of binding sites within the chitosan–carbon nanoparticle film is controlled by changing the thickness of the film deposit or by changing the chitosan content, which is varied by changing the chitosan concentration during layer-by-layer deposition. Voltammetric characteristics and stability of the chemisorbed and physisorbed redox systems are reported as a function of pH. The physisorbed redox system is expelled from the film at a pH consistent with the pK_A of chitosan (approximately 6.5). However, the 2-methyleneanthraquinone redox system remains stable even in alkaline media and only a minor inflection in the plot of midpoint potentials *vs.* pH indicates the film deprotonation process at the pK_A of chitosan.

1 Introduction

Chitosan is a biopolymer, poly-(β-1-4)-2-amino-2-deoxy-D-glucopyranose, produced by partial alkaline *N*-deacetylation of chitin, which can be widely found in the exoskeleton of shellfish and crustaceans as the second most abundant natural biopolymers next to cellulose.[1] Chitosan is a cationic polyelectrolyte (with pK_a ≈ 6.5[2]), soluble in acidic aqueous media, and it forms water insoluble complexes for example with anionic polyelectrolytes.[3] Chitosan, as an environment-friendly and cost-effective material, has received considerable research attention over the recent years and applications have been proposed in particular in the removal of heavy metals[4–8] based on an excellent chitosan-metal binding capacity. Also, the use of chitosan in sensor systems[9] and modified electrodes[10,11] has been reported. The solubility of chitosan in aqueous acidic solutions and the presence of hydroxyl and amino functional groups are features which aid the physical and chemical modification of chitosan and the formation of chitosan-based membranes in a variety of configurations, *e.g.* beads, membranes, coatings, capsules, fibers and sponges.[12]

Carbon materials are widely used in electroanalysis[13] and recently the benefits of nano-carbons and fullerenes has been a trigger of new developments in the design of modified electrodes for electrochemical sensing.[14] Carbon nanoparticles similar to metal nanoparticles[15] are very interesting high surface area building blocks in thin film electrode systems and their high content of interfacial edge sites are potentially beneficial in electrochemical processes. Surface functionalized carbon nanoparticles have been proposed for applications such as antioxidant adsorption[16] and stabilizer adsorption.[17] The use of chemically surface-modified (tosylated) carbon nanoparticles with negative surface charge as hydrophilic building blocks in the layer-by-layer assembly of thin carbon composite films has been reported recently for the polycationic binder poly(diallyldimethylammonium chloride)[18,19] and is explored here for the chitosan binder system.

The layer-by-layer (LbL) assembly technique[20] provides an easy, low-cost, and versatile method for the fabrication of simple or stratified films, and here for the chitosan-based electrodes. Briefly, this technique is based on the alternating adsorption of oppositely charged polyelectrolytes onto a charged substrate.[21] The major advantage of the layer-by-layer technique is its thickness control and introduction of diverse chemical functionality. By virtue of the electrostatic attraction of oppositely charged molecules, chitosan, owing to its cationic polyelectrolyte nature in acidic conditions, spontaneously forms water-insoluble complexes with anionic polyelectrolyte[22–24] and it is used here in the assembly of negatively charge carbon nanoparticles from an aqueous colloidal suspension.

In the present study, the layer-by-layer assembly process is used to grow thin carbon nanoparticle (CNP) films with approximately 2 nm per layer average thickness increase and variable composition. The resulting chitosan–CNP films are modified with redox systems (i) *via* physisorption of indigo carmine and (ii) *via* chemisorption of 2-methyleneanthraquinone. The binding of these redox systems and the stability of voltammetric responses as a function of pH are investigated. The use of layer-by-layer deposited carbon nanoparticle–chitosan film electrodes is novel and in future physical and chemical modification of these electrodes may help in developing new fast and sensitive sensor electrodes.

[a] *Laboratory of Applied Environmental Chemistry, Department of Environmental Sciences, University of Kuopio, Patteristonkatu 1, 50101 Mikkeli, Finland*
[b] *Department of Chemistry, University of Bath, Claverton Down, Bath, UK BA2 7AY. E-mail: F.Marken@bath.ac.uk*

2 Experimental

2.1 Chemical reagents

Surface-tosylated carbon nanoparticles (water-soluble, *ca.* 8 nm average diameter, Emperor 2000) were obtained from Cabot Corporation, chitosan (poly-D-glucosamine, low molecular weight, 75–85% deacetylated), indigo carmine (5,5′-indigodisulfonic acid, disodium salt), acetic acid, NaOH, K_2HPO_4, KH_2PO_4, and 2-bromomethylanthraquinone were obtained from Aldrich or Fluka and used without further purification. De-ionised and filtered water was taken from an Elgastat water purification system (Elga, High Wycombe, Bucks) with a resistivity of not less than 18 MΩ cm. Argon (BOC, Pureshield) was employed to de-aerate solutions. All experiments were performed at $T = 20 \pm 2$ °C.

2.2 Instrumentation

A microAutolab III potentiostat system (EcoChemie, Netherlands) was employed for voltammetric studies with a Pt gauze counter electrode and a KCl-saturated calomel (SCE) reference electrode (Radiometer, Copenhagen). The working electrode was prepared from ITO coated glass (tin-doped indium oxide films sputter-coated onto glass, active area 10 mm × 10 mm, resistivity 15 Ω per square) obtained from Image Optics Components Ltd (Basildon, Essex, UK). The ITO electrodes were rinsed with acetone and water, heat treated in a tube furnace (Elite Thermal Systems Ltd) for 1 h at 500 °C, and re-equilibrated to ambient conditions before use. Voltammograms were recorded in staircase mode (0.45 mV step potential). Atomic force microscopy (AFM) images were obtained with a Digital Instruments Nanoscope IIIa Multi-Mode Scanning Probe Microscope in the AFM contact mode.

2.3 Procedure I: layer-by-layer formation of chitosan–CNP films at ITO electrodes

A layer-by-layer deposition strategy was chosen to prepare thin layer electrodes on ITO substrates. An aqueous suspension of carbon nanoparticle (1 mg in 10 cm^3 deionised water, sonicated) and a solution of 0.35 wt% chitosan (0.35 g of the low molecular weight biopolymer in 6 cm^3 conc. acetic acid, diluted to 100 cm^3, and adjusted with NaOH to pH 5) were prepared separately. For deposition to occur the ITO electrode was dipped first into the chitosan solution for 30 s, rinsed with water, and then it was dipped into the carbon nanoparticle solution for 30 s, and rinsed with water. This procedure was repeated to build up multi-layer thin film electrodes.

2.4 Procedure II: physisorption into chitosan–CNP thin film electrodes

Indigo carmine was physisorbed into a chitosan–carbon nanoparticle thin film by 20 min immersion into aqueous 1 mM indigo carmine (unless stated otherwise) in 0.1 M phosphate buffer pH 2. Then electrodes were rinsed with de-ionised water, transferred into a clean phosphate buffer solution, and used for measurements.

2.5 Procedure III: chemisorption into chitosan–CNP thin film electrodes

2-Methyleneanthraquinone was chemisorbed into chitosan–carbon nanoparticle electrodes by first pretreating the electrode in aqueous 1 M NaOH solution, followed by rinsing with water and drying, and 20 min immersion into 1 mM 2-bromomethylanthraquinone in acetonitrile. The electrode is then rinsed with acetonitrile and dried, and finally transferred into the aqueous buffer solution for voltammetric measurements.

3 Results and discussion

3.1 Layer-by-layer formation of chitosan–CNP thin film deposits at ITO electrodes

The layer-by-layer formation of chitosan–CNP films on tin-doped indium oxide (ITO) substrates is evident from the change from a clear to black coloration during the deposition

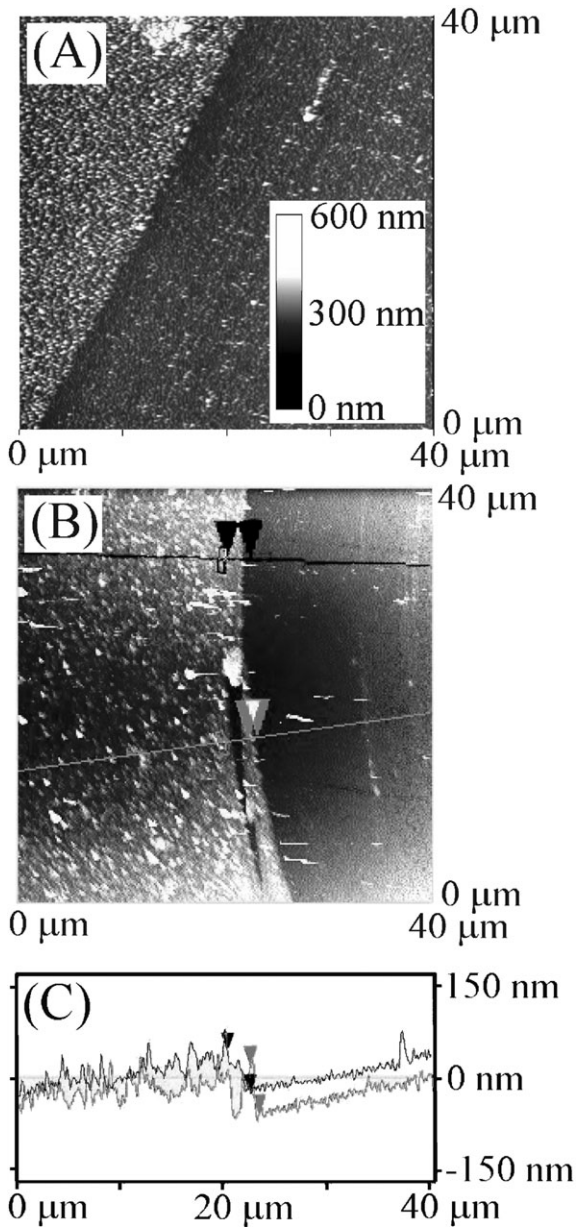

Fig. 1 AFM images of (A) a 20-layer chitosan–CNP film and (B) a 40-layer chitosan–CNP film with a scratch revealing the underlying substrate. (C) Cross-sectional height analysis showing that a single layer is adding only approximately 2 nm thickness.

process and the layer-by-layer formation of a very thin film is confirmed in AFM images (see Fig. 1).

Fig. 1(A) shows a 20-layer deposit with part of the film removed with a scalpel. Fig. 1(B) and (C) show a 40-layer film in topography and in cross section and the typical average height of *ca.* 80 nm is consistent with an average increase in thickness of *ca.* 2 nm in each chitosan–CNP deposition cycle. This rate of deposition is considerably less than that observed with the poly(diallyldimethylammonium chloride) binder in CNP–PDDAC films reported recently.[20] However, the film formation is uniform and reproducible and therefore CNP–chitosan multi-layer films are of sufficient quality for further investigation and application.

In order to explore the electronic properties of the chitosan–CNP multilayer films at ITO electrode surfaces cyclic voltammograms in aqueous 0.1 M phosphate buffer pH 7 were obtained (see Fig. 2).

Voltammetric responses show a clear capacitance contribution from the carbon nanoparticle deposit. With increasing number of deposition cycles an approximately linear increase in capacitance (see Fig. 2(B)) is observed. The deposition process was repeated with different chitosan concentration during deposition (0.001, 0.01, 0.02, 0.04 and 0.35 wt% chitosan) and essentially identical changes in capacitance are observed independent of the chitosan concentration during deposition. It seems likely that (during the short deposition period of 30 s) the amount of carbon nanoparticles adhering to the surface of the growing chitosan–CNP film is governed by the electrostatic binding to the surface without effects of chitosan depth or surface concentration (*vide infra*).

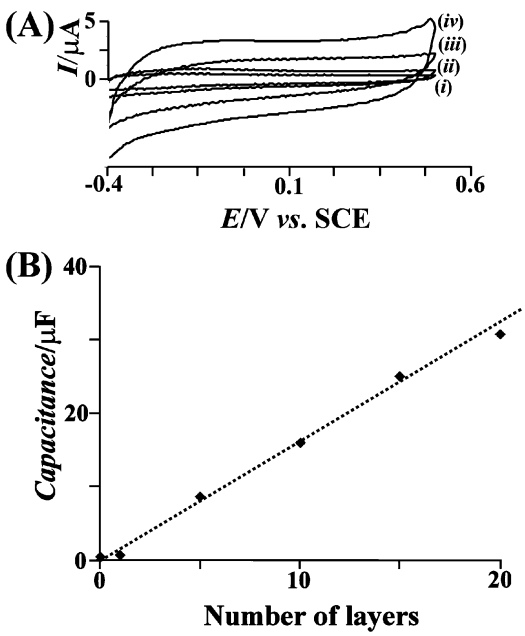

Fig. 2 (A) Cyclic voltammograms (scan rate 0.1 V s^{-1}, geometric area *ca.* 1 cm^2) for (i) 0-layer, (ii) 1-layer, (iii) 10-layer and (iv) 20-layer chitosan–CNP immersed in aqueous 0.1 M phosphate buffer pH 7. (B) Plot of the capacitance (determined from cyclic voltammograms) *vs.* the number of deposition cycles (see Experimental section).

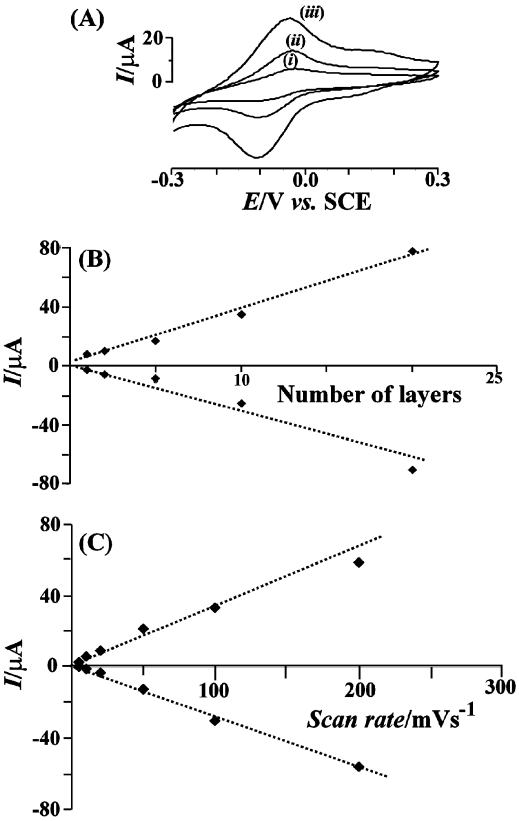

Fig. 3 (A) Cyclic voltammograms (scan rate 0.1 V s^{-1}, area 1 cm^2) for the reduction and re-oxidation of indigo carmine adsorbed into a (i) 2-layer, (ii) 5-layer and (iii) 10-layer chitosan–CNP film deposit immersed in aqueous 0.1 M phosphate buffer pH 2 (immobilisation of indigo carmine by immersion into 1 mM indigo carmine in 0.1 M phosphate buffer pH 2). (B) Plot of the peak current *vs.* the number of chitosan–CNP deposition layers. (C) Plot of the peak current *vs.* scan rate for a 10-layer chitosan–CNP film immersed in 0.1 M phosphate buffer pH 2 (immobilisation of indigo carmine by immersion into 1 mM indigo carmine in 0.1 M phosphate buffer pH 2).

3.2 Physisorption of indigo carmine into chitosan–CNP thin film electrodes

For the adsorption of a negatively charged redox probe into the chitosan–CNP film binding *via* physisorption is anticipated as long as the solution pH is sufficiently acidic to maintain ammonium functionality in the chitosan–CNP film. Here, indigo carmine, a well known reversible two-electron–two-proton redox system,[25,26] is employed to probe the chitosan binding sites.

Adsorption of indigo carmine was achieved by 20 min immersion of the film electrode into 1 mM indigo carmine in 0.1 M phosphate buffer pH 2 (see Experimental section). When transferred into clean 0.1 M phosphate buffer pH 2, voltammetric responses for the reduction and re-oxidation of indigo carmine are observed at −0.07 V *vs.* SCE (see Fig. 3(A)). The voltammetric response is dependent on the number of deposition cycles applied during thin film formation (see Fig. 3A) and a plot of the peak current as a function of film thickness is shown in Fig. 3(B). The increase in voltammetric response is approximately linear up to at least 20-layer films and does probably further increase beyond this point. Deviation from linearity are expected in thicker films (*ca.* 1–2 μm) when diffusion effects and buffer limitations arise.[27]

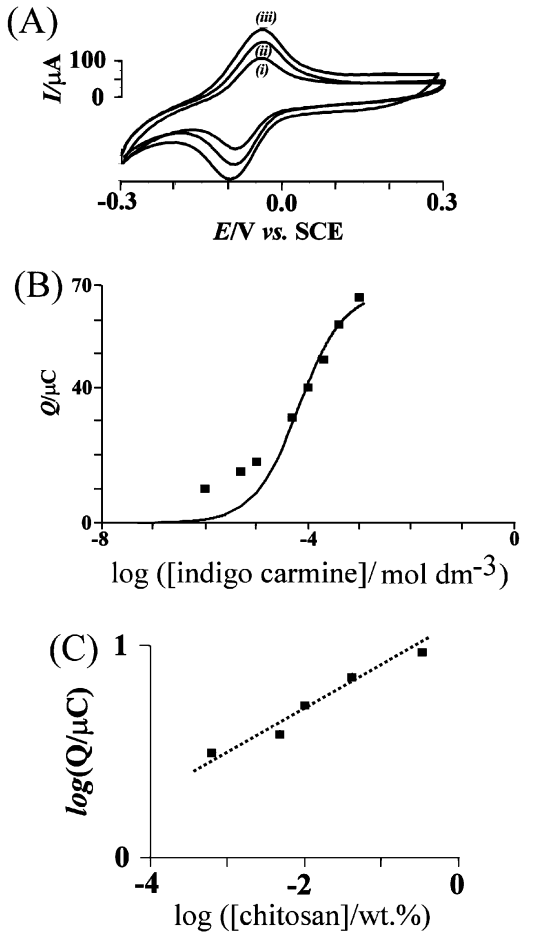

Fig. 4 (A) Cyclic voltammograms (scan rate 0.1 V s^{-1}, area 1 cm^2) for a 10-layer chitosan–CNP on ITO (pretreated by immersion in (i) 5 μM, (ii) 20 μM and (iii) 100 μM indigo carmine for 20 min) immersed in 0.1 M phosphate buffer pH 2. (B) Langmuir isotherm plot for the immobilization of indigo carmine into a chitosan–CNP film. The line corresponds to a binding constant $K_{\text{indigo carmine}} = 15\,000\ \text{mol}^{-1}\ \text{dm}^3$. (C) Plot of the charge under the peak current for indigo carmine (for a 10-layer chitosan–CNP film on ITO pretreated in 1 mM indigo carmine in 0.1 M phosphate buffer pH 2) *vs.* the deposition concentration of chitosan during layer-by-layer coating (see Experimental section).

The peak current is also increasing proportionally with scan rate (see Fig. 3(C)) consistent with a thin layer of fully active redox active material immobilized at the electrode surface.

Next, the binding ability of indigo carmine into the chitosan–CNP host is investigated. Fig. 4(A) shows typical voltammetric responses obtained with a 10-layer chitosan–CNP film after pretreatment in aqueous solutions of different indigo carmine content. A clear transition in the peak current is observed at a concentration of approximately 100 μM indigo carmine and the analysis of the plot in terms of a Langmuir isotherm suggests an approximate binding constant of $K_{\text{indigo carmine}} = 1.5 \times 10^4\ \text{mol}^{-1}\ \text{dm}^3$ (which is consistent but weaker when compared with previous literature reports for binding into a poly(diallyldimethylammonium) composite[18]).

Interestingly, the amount of chitosan within the layer-by-layer deposit can be altered by varying the concentration of chitosan during the deposition. Fig. 4(C) shows a plot of the charge under the indigo carmine redox response (for a 10-layer deposit, pretreatment in 1 mM indigo carmine, scan rate 0.1 V s^{-1}) *vs.* the chitosan concentration during deposition. A non-linear trend (exponent ≈ 0.2) with an increasingly dramatic effect at lower chitosan concentration is observed. In contrast, no change in the amount of carbon nanoparticles is observed (*vide supra*) and therefore probably additional coiling of chitosan or more rapid surface-binding of poly-electrolyte at higher chitosan concentration is responsible for the compositional and binding site change.

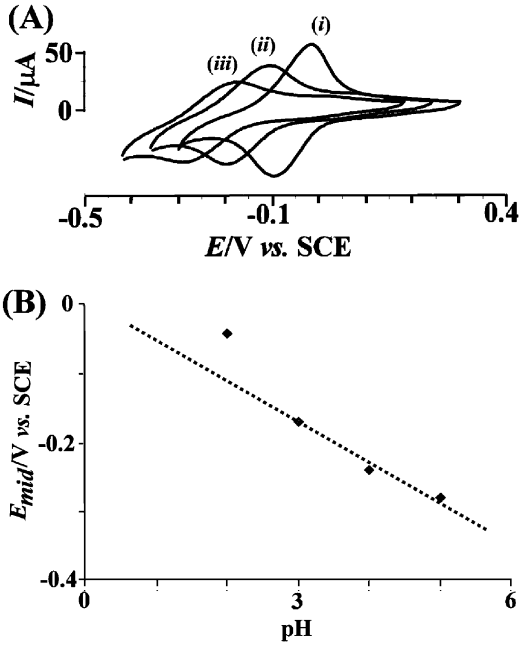

Fig. 5 (A) Cyclic voltammograms (scan rate 0.1 V s^{-1}, area 1 cm^2) for a 10-layer chitosan–CNP film electrode (pretreated in 1 mM indigo carmine in 0.1 M phosphate buffer pH 2) immersed in 0.1 M phosphate buffer at (i) pH 2, (ii) pH 3, and (iii) pH 4. (B) Plot of the midpoint potential $E_{\text{mid}} = 1/2(E_p^{\text{ox}} + E_p^{\text{red}})$ *vs.* pH in 0.1 M phosphate buffer solution. The dotted line corresponds to a 59 mV slope.

The effect of the solution pH on the voltammetric response is studied next. Fig. 5(A) shows typical cyclic voltammograms obtained for the reduction and re-oxidation of indigo carmine at pH 2, 3 and 4. A shift of the midpoint potential to more negative values occurs at lower proton activity approximately consistent with the Nernstian shift (see Fig. 5(B)) expected for the indigo carmine redox system. In addition, the shape of the voltammetric response is changing and broader signals are observed as the pH is increased. No more voltammetric signals for the indigo carmine reduction are observed at pH >6 consistent with the loss of positively charged ammonium binding sites for indigo carmine. The change in shape at pH 3 and 4 is likely to be related to the local pH within the chitosan–CNP film and changes in the buffer capacity of the phosphate buffer.

The electrochemical properties of the indigo carmine physisorbed into the chitosan–CNP film electrode are dominated by the state of protonation of the glucosamine functionality. It is interesting to compare the voltammetric characteristics of the physisorbed indigo carmine and a chemisorbed redox system such as 2-methyleneanthraquinone.

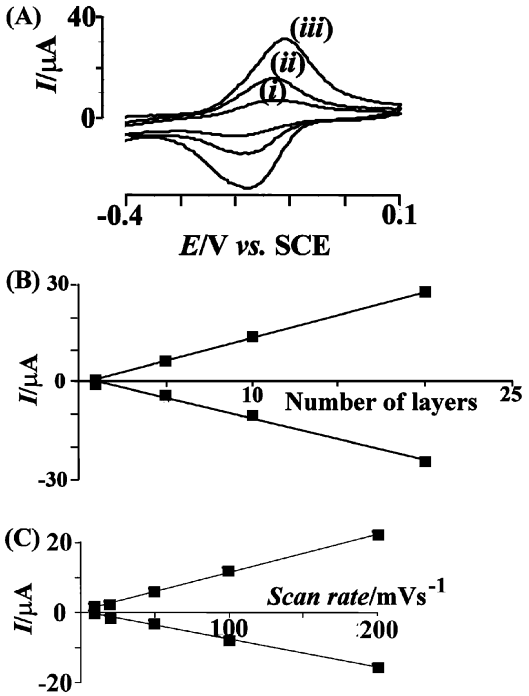

Fig. 6 (A) Cyclic voltammograms (scan rate 0.1 V s^{-1}, area 1 cm^2) for chitosan–CNP modified ITO electrode (pretreated for 20 min in 1 mM 2-bromomethylanthraquinone in acetonitrile, see Experimental section) immersed in 0.1 M phosphate buffer solution pH 2 for a different number of deposition layers: (i) 5, (ii) 10 and (iii) 20 layers. (B) Plot of the peak current for 2-methyleneanthraquinone chemisorbed into chitosan–CNP *vs.* the number of layers. (B) Plot of the peak current for chemisorbed 2-methyleneanthraquinone (for a 10-layer chitosan–CNP film on ITO pretreated in 1 mM 2-bromomethylanthraquinone in acetonitrile for 20 min, see Experimental section) immersed in 0.1 M phosphate buffer pH 2 *vs.* the scan rate.

3.3 Chemisorption of 2-methyleneanthraquinone into chitosan–CNP thin film electrodes

Anthraquinone is a well known two-electron–two-proton redox system[28] which has been used as a catalyst for the reduction of oxygen[29] or as a pH sensitive redox probe.[30] Anthraquinone derivatives can be immobilized onto suitable electrode surface by physisorption (*e.g.* by solvent evaporation[31]) or by chemisorption (usually based on diazonium coupling redox chemistry[32]). Chemisorption has been shown to lead to superior stability[33] and it is shown here that chemisorption of 2-methyleneanthraquinone can be achieved by a simple C–N coupling process in acetonitrile media. 2-Bromomethylanthraquinone is dissolved in acetonitrile (typically 1 mM) and a dry chitosan–CNP film electrode (deprotonated by pretreatment in 0.1 M NaOH, see experimental) is immersed for 20 min. After rinsing with acetonitrile and drying, the electrode is transferred into an aqueous buffer solution (0.1 M phosphate buffer pH 2) and a new reversible voltammetric response is observed at −0.15 V *vs.* SCE (see Fig. 6(A)). The new voltammetric response can be identified as the two-electron–two-proton reduction of anthraquinone[34] and a plot of the peak current *vs.* the number of deposition layers clearly demonstrates the binding into the chitosan–CNP film (see Fig. 6(B)). The effect of scan rate on the voltammetric peak current (see Fig. 6(C)) is consistent with a fully redox active thin film deposit.

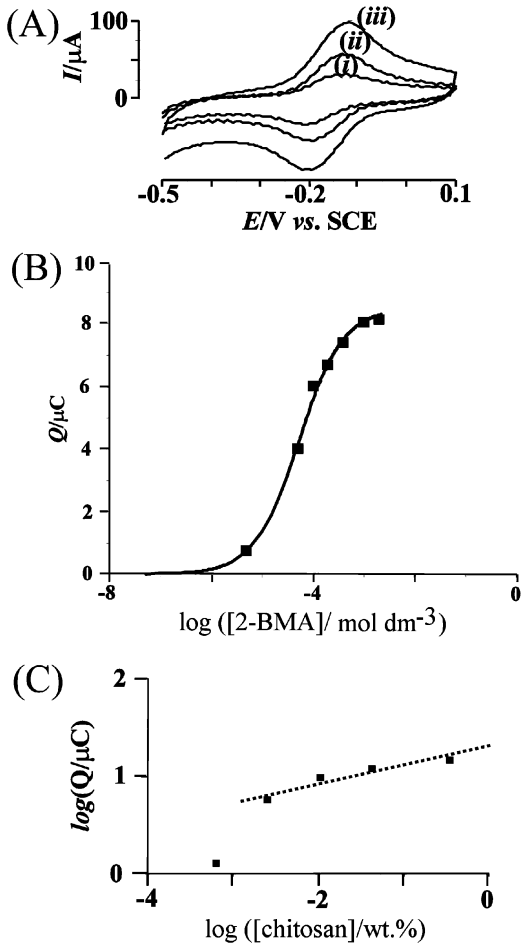

Fig. 7 (A) Cyclic voltammograms (scan rate 0.1 V s^{-1}, area 1 cm^2) for a 10-layer chitosan–CNP film electrode (pretreated with (i) 50, (ii) 100, and (iii) 200 μM 2-bromomethylanthraquinone in acetonitrile, see Experimental section) immersed in 0.1 M phosphate buffer pH 2. (B) Langmuir isotherm plot for the immobilization of 2-methyleneanthraquinone into a chitosan–CNP film. The line corresponds to an approximate binding constant $K_{\text{2-methyleneanthraquinone}}$ = 19 000 mol^{-1} dm^3. (C) Plot of peak charge for oxidation of immobilized 2-methyleneanthraquinone (after pretreatment of a 10-layer chitosan–CNP film electrode in 1 mM 2-bromomethylanthraquinone) immersed in 0.1 M phosphate buffer pH 2 *vs.* the chitosan concentration during layer-by-layer deposition.

Voltammograms shown in Fig. 7(A) demonstrate the effect of the 2-bromomethylanthraquinone concentration during the chemisorption process. Clearly, a decrease in the amount of bound anthraquinone occurs at lower 2-bromomethylanthraquinone concentration. A plot of the charge under the reduction peak *vs.* the concentration of 2-bromomethylanthraquinone shows typical Langmuir isotherm characteristics and a binding constant, $K_{\text{2-methyleneanthraquinone}}$ = 1.9×10^4 mol^{-1} dm^3, can be estimated (see Fig. 7(B)).

The effect of the chitosan concentration during the deposition process is shown in Fig. 7(C). The trend is very similar to that observed for indigo carmine physisorption although at lower chitosan concentration a more dramatic loss of binding ability occurs. The effect of the solution pH on the voltammetric response for immobilized 2-methyleneanthraquinone is considerably different from that observed for immobilised

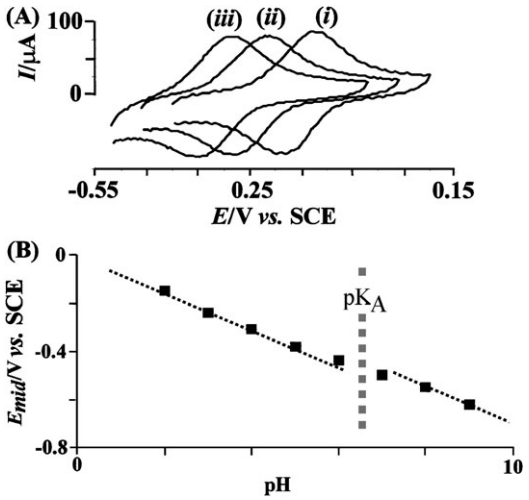

Fig. 8 (A) Cyclic voltammograms (scan rate 0.1 V s^{-1}, area 1 cm^2) for a 10-layer chitosan–CNP film electrode (pretreated in 1 mM 2-bromomethylanthraquinone in acetonitrile, see Experimental section) immersed in 0.1 M phosphate buffer at pH (i) 2, (ii) 3 and (iii) 4. (B) Plot of the midpoint potential $E_{mid} = 1/2(E_p^{ox} + E_p^{red})$ for reduction and re-oxidation of 2-methyleneanthraquinone immobilized in a 10-layer chitosan–CNP film *vs.* the pH in 0.1 M phosphate buffer solution (the dotted line indicates a slope of 59 mV).

indigo carmine. Fig. 8(A) shows a set of voltammograms obtained at pH 2, 3 and 4 and it can be seen that the voltammetric signal is stable and a well-defined shift in midpoint potential occurs with pH. The plot of the midpoint potential *vs.* pH (see Fig. 8(B)) is consistent with virtually ideal Nernstian behaviour over a 2 to 10 pH range. A minor inflection in the plot occurs at pH 6–7 due to the deprotonation of chitosan causing a secondary effect on the reversible potential of the anthraquinone redox system. The pK_A of the chitosan–CNP film can be estimated as 6.5 in good agreement with literature reports for pure chitosan.[35]

The stable voltammetric response for the anthraquinone-derivatised chitosan–CNP film electrode is promising and similar films will be potentially useful in application requiring stable pH measurements or in electrocatalysis. In future, similarly chemisorption-derivatised chitosan–CNP film electrodes will be of interest in a wider range of sensor and analytical applications.

4 Conclusions

A layer-by-layer strategy has been employed in order to deposit thin carbon nanoparticle films onto ITO substrates. The binder chitosan is shown to effectively bind and electrically connect the carbon film. The chitosan binder also is shown to provide binding sites for physisorption (for dianionic indigo carmine) and for chemisorption (of 2-methyleneanthraquinone *via* reaction with 2-bromomethylanthraquinone). Chemisorption and physisorption are believed to occur both at the amine functionality but are independent and therefore possible simultaneously. The chemisorbed redox system provides a much more stable and versatile electrode which is responding over a wide pH range without deterioration in the alkaline pH range. By changing the chitosan concentration during deposition, the number of glucosamine binding sites could be controlled.

Acknowledgements

The authors would like to thank the EU and TEKES, Finnish Funding Agency for Technology and Innovation, for financial support of this work. We thank Hugh Perrott (Department of Physics, Bath) for help with AFM imaging. Support from Cabot Corporation with Emperor 2000 carbon nanoparticle materials is gratefully acknowledged.

References

1. See, for example: R. Jayakumar, N. Nwe, S. Tokura and H. Tamura, *Int. J. Biol. Macromol.*, 2007, **40**, 175.
2. H. Sashiwa, Y. Shigemasa and R. Roy, *Chem. Lett.*, 2000, **29**, 596.
3. N. Kubota, Y. Kikuchi, Macromolecular complexes of chitosan, , in *Polysaccharides*, ed. S Dumitriu, Marcel Dekker, New York, pp. 595–628.
4. C. L. Schauer, M. S. Chen, R. R. Price, P. E. Schoen and F. S. Ligler, *Environ. Sci. Technol.*, 2004, **38**, 4409.
5. V. M. Boddu, K. Abburi, J. L. Talbott and E. D. Smith, *Environ. Sci. Technol.*, 2003, **37**, 4449.
6. K. H. Chu, *J. Hazard. Mater. B*, 2002, **90**, 77.
7. E. Onsoyen and O. Skaugrud, *J. Chem. Technol. Biotechnol.*, 1990, **49**, 395.
8. R. S. Vieira and M. M. Beppu, *Colloids Surf., A*, 2006, **279**, 196.
9. See for example: D. Du, J. W. Ding, J. Cai and A. D. Zhang, *Sens. Actuators, B*, 2007, **127**, 317.
10. Q. M. Zhou, Q. J. Xie, Y. C. Fu, Z. H. Su, X. Jia and S. Z. Yao, *J. Phys. Chem. B*, 2007, **111**, 11276.
11. D. Du, J. W. Ding, J. Cai and A. D. Zhang, *Colloids Surf., B*, 2007, **58**, 145.
12. B. Krajewska, *Sep. Purif. Technol.*, 2005, **41**, 305.
13. G. G. Wildgoose, C. E. Banks, H. C. Leventis and R. G. Compton, *Microchim. Acta*, 2006, **152**, 187.
14. C. E. Banks and R. G. Compton, *Anal. Sci.*, 2005, **21**, 1263.
15. C. W. Welch and R. G. Compton, *Anal. Bioanal. Chem.*, 2006, **384**, 601.
16. J. M. Pena, N. S. Allen, M. Edge, C. M. Liauw and B. Valange, *Polym. Degrad. Stab.*, 2001, **72**, 31.
17. J. M. Pena, N. S. Allen, C. M. Liauw, M. Edge, B. Valange and S. Santamaria, *J. Mater. Sci.*, 2001, **36**, 4443.
18. M. Amiri, S. Shahrokhian and F. Marken, *Electroanalysis*, 2007, **19**, 1032.
19. M. Amiri, S. Shahrokhian, E. Psillakis and F. Marken, *Anal. Chim. Acta*, 2007, **593**, 117.
20. G. Decher and J. B. Schlenoff, *Multilayer Thin Films*, Wiley–VCH, Weinheim, 2003.
21. K. J. McKenzie, F. Marken, M. Hyde and R. G. Compton, *New J. Chem.*, 2002, **26**, 625.
22. S. Dumitriu and E. Chornet, *Adv. Drug Delivery Rev.*, 1998, **31**, 223.
23. K. Singla and M. Chawla, *Pharm. Pharmacol. Lett.*, 2001, **53**, 1047.
24. D. Magnin, S. Dumitriu and E. Chornet, *J. Bioact. Compat. Polym.*, 2003, **18**, 355.
25. S. C. Mo, J. M. Na, H. Mo and L. Chen, *Anal. Lett.*, 1992, **25**, 899.
26. Y. J. Li and S. J. Dong, *J. Electroanal. Chem.*, 1993, **348**, 181.
27. L. Rassaei, M. Sillanpää and F. Marken, *Electrochim. Acta*, submitted.
28. A. Salimi, C. E. Banks and R. G. Compton, *Phys. Chem. Chem. Phys.*, 2003, **5**, 3988.
29. C. E. Banks, G. G. Wildgoose, C. G. R. Heald and R. G. Compton, *J. Iran. Chem. Soc.*, 2005, **2**, 60.
30. I. Streeter, H. C. Leventis, G. G. Wildgoose, M. Pandurangappa, N. S. Lawrence, L. Jiang, T. G. J. Jones and R. G. Compton, *J. Solid State Electrochem.*, 2004, **8**, 718.
31. J. S. Xu, Q. Y. Chen and G. M. Swain, *Anal. Chem.*, 1998, **70**, 3146.
32. A. Sarapuu, K. Helstein, D. J. Schiffrin and K. Tammeveski, *Electrochem. Solid-State Lett.*, 2005, **8**, E30.
33. B. Sljukic, C. E. Banks and R. G. Compton, *Electroanalysis*, 2005, **17**, 1025.
34. G. G. Wildgoose, M. Pandurangappa, N. S. Lawrence, L. Jiang, T. G. J. Jones and R. G. Compton, *Talanta*, 2003, **60**, 887.
35. H. Sashiwa, Y. Shigemasa and R. Roy, *Chem. Lett.*, 2000, **29**, 596.

